

12.4 STRONG WIND SHEARS IN STRATIFORM PRECIPITATION OBSERVED WITH WEATHER RADAR

V. M. Melnikov and R. J. Doviak

*Cooperative Institute for Mesoscale Meteorological Studies, University of Oklahoma and
NOAA/OAR National Severe Storms Laboratory, Norman, Oklahoma*

1. Introduction

Weather radars are used in aviation meteorology to monitor potential wind hazards. Two parameters (i.e., the Doppler velocity and spectrum width) measured with weather radars are connected to accelerations that possibly can affect safety of flight (e.g., Mahapatra 2000, Bieringer et al., 2004). The spectrum widths, SW, larger than 4 m s^{-1} are used to indicate the potential hazard to aircraft and/or its crew and passengers (e.g., Lee 1977, Mahapatra 2000). Airplanes are mostly affected by the along-track gradients of the vertical wind (Proctor, et al., 2002), a component typically not measured with airborne or ground-based weather radars. Fortunately, good correlation between the variance of vertical and along track wind components has been observed in strong convection (Hamilton and Proctor 2006a, b). In thunderstorm environments, Lee (1977), Bohne (1981), Meischner et al. (2001), and Cornman et al. (2003) found strong correlation between aircraft shocks and large SW measured by airborne and/or ground-based weather radars. We call SW “large” if it equals or exceeds 4 m s^{-1} . The threshold of 4 m s^{-1} is used because it is accepted as an indicator of turbulence possibly hazardous to aircraft and/or its crew (Lee, 1977; Evans, 1985).

In stratiform precipitation, median SWs lie in an interval between 1 and 3 m s^{-1} (Fang 2003, Fang et al. 2004). On the other hand, median SW in thunderstorms and squall lines are in a 3 to 6 m s^{-1} interval (Fang et al., 2004). Our observations, of SW fields in stratiform precipitation in central Oklahoma, also exhibit median widths of 1 to 3 m s^{-1} , but often we find vast areas of exceptionally large SW (i.e., larger than 4 and even 10 m s^{-1}

which is the largest width measured in thunderstorms). Our radar observations in stratiform precipitation exhibit layered patterns of large SWs in contrast to convective environment where large SW have spotty patterns corresponding to areas with strong convection (updrafts), downdrafts, the areas between up- and downdrafts, as well as tornadic circulations. So our first goal is to collect preliminary statistics on large spectrum widths in stratiform precipitation. We show that areas of large spectrum widths contain strong shear of mean wind. Our second goal is the estimation of mean wind shear. We analyze three approaches based on: 1) measurements of gradients of the Doppler velocity in two radar volumes spaced in height, 2) measurements of the gradients of the velocity along slant radial, 3) spectrum width measurements.

2. Patterns of the Doppler velocity and spectrum width fields in stratiform precipitation

We present herein radar data collected with the NSSL’s Research & Development WSR-88D KOUN (11-cm wavelength, 3-dB one-way beamwidth is 0.95° , range resolution is 250 m, pulse repetition frequencies were 1013 or 1280 Hz). Radar images are presented in two formats: 1) a slant circular section called a Plan Position Indicator (PPI), and 2) a vertical cross-section called a Range Height Indicator (RHI). All RHIs herein are obtained from elevation scans, not constructed from a collection of PPIs made at different elevation angles. An example of reflectivity factor and SW fields in the PPI format is presented in Fig. 1 which is typical of patterns in widespread precipitations (i.e., Z, less than 40 dBZ, and SWs less than 4 m s^{-1}).

Valery.Melnikov@noaa.gov

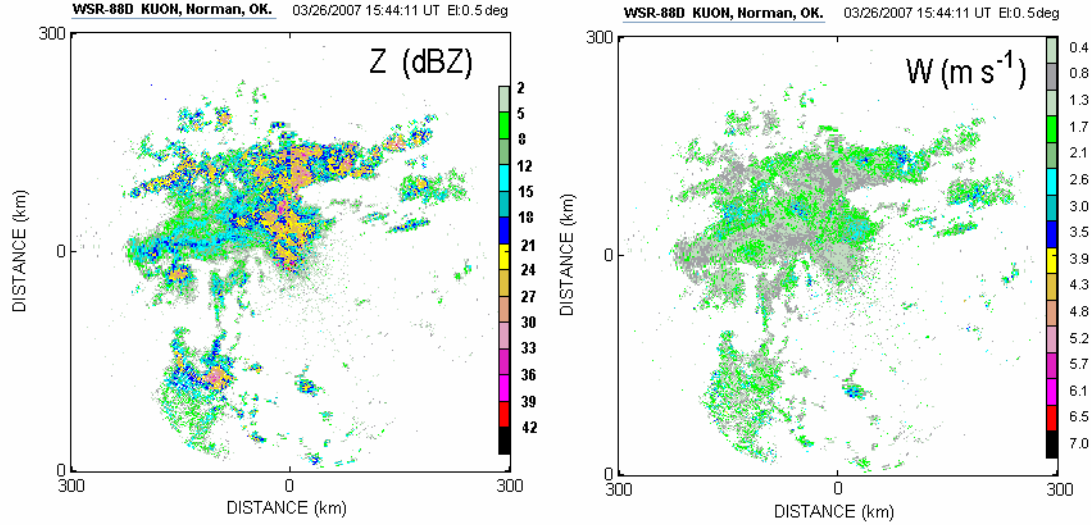


Fig 1. PPI images of (left) reflectivity factor (Z) and (right) the spectrum width (W) on March 26, 2007 at 1544 UT, and elevation 0.5° .

A general rule-of-thumb in preventing aircraft accidents is to avoid areas of reflectivity factors larger than 40 dBZ (Hamilton and Proctor, 2006). Measurements (Lee and Carpenter, 1979) of turbulence with aircraft penetrations in and around thunderstorms suggest that pilots can avoid moderate or stronger turbulence by staying more than 15 km away from the 40 dBZ region of convective storms. Hamilton and Proctor (2002, 2006), and Cornman et al. (2003) have shown that moderate turbulence can be located in zones near thunderstorms, but in regions having significantly lower reflectivities (i.e., 5-15 dBZ), in agreement with the earlier findings of Lee and Carpenter (1979). Based on this rule we can conclude that situation in Fig. 1 is safe for flights because Z is less than 40 dBZ. This is supported by the SW (W) field. It should be noted that there is no correlation between the Z and SW fields.

We have analyzed Z and SW fields in stratiform precipitation in cold seasons of 2001 to 2006 and noticed that SW fields often contain areas of very wide spectra. Our radar data on 87 days with stratiform precipitation contain areas with $SW > 4 \text{ m s}^{-1}$ in 75 cases. Some data statistics are presented in Table 1. Maximal measured SWs are denoted as $\sigma_{v \text{ max}}$ in the table. Often, SW fields have layered patterns on RHIs. In more than 40% of the days that were analyzed, areas of large SW were located in the lowest kilometer above the ground, i.e., in the layer wherein airplanes ascend and descend. To reveal layered structures in SW fields, we first observed data on a PPI display, and then made elevation angle (RHI) scans through areas of enhanced SW. We found that reconstruction of the layered structures, from a collection of PPIs with beam width separation in elevation, is frequently impossible because of the small thickness of the layers. For that reason most of images presented herein were collected and displayed in a vertical scan (RHI) mode.

Table 1. Statistics of SW measurements collected on 87 days having stratiform precipitation in the cold seasons of 2001 to 2006.

	$\sigma_{v \text{ max}} < 4 \text{ m s}^{-1}$	$\sigma_{v \text{ max}} \geq 7 \text{ m s}^{-1}$	Layered, $\sigma_{v \text{ max}} > 4 \text{ m s}^{-1}$	Altitude $< 1 \text{ km}$, $\sigma_{v \text{ max}} > 4 \text{ m s}^{-1}$
Number of cases (%)	12 (14%)	37 (43%)	67 (77%)	37 (43%)

It is seen from the table that in more than 70% of cases layered patterns of SW have been observed. Such patterns are clearly seen on RHI displays in Fig. 2. The data were collected with the elevation step of 0.2° which is only one fifth of the antenna beamwidth. Heights indicated in the RHI displays are above the radar horizon. Largest SWs measured in cases Fig. 2 (a), (b), and (c) are 9, 13, and 16 m s^{-1} correspondingly, much larger than the threshold of 4 m s^{-1} for moderate to severe turbulence. In thunderstorms, according to Fang et al. (2004), largest SWs are about 10 m s^{-1} . The maximal SWs in Figs. 2 (b) and (c) are larger than those maximal SW in thunderstorms. Fang (2003) has reported SWs $> 7 \text{ m s}^{-1}$ are found a few places, but principally in the upper regions of thunderstorms. On the other hand, such large widths constitute more than 40% of the observations in stratiform precipitation (Table 1).

The Doppler velocity fields show that layers of large widths coincide with areas of the strong vertical gradients of Doppler velocities (e.g., Fig 2 (d, e, f)). That is, mean wind shear is a strong contributor to spectrum widths. Estimation of mean wind shear is discussed in the next section.

Layers of large SW can be located near the ground (Fig. 2 b, c). In such cases, it is difficult to restore the vertical structure of the layers from PPI scans collected with existing Volume Coverage Patterns, VCPs, on the WSR-88D. Two lowest elevations of VCP11 (El= 0.5° and 1.45°) are shown with the black lines in Figs. 2 b, c. It is seen that the layers are located below El= 1.45° . Fig. 2 also demonstrates that the dense elevation sampling restores the fine vertical structures of the layers.

The “rule-of-thumb” does not work in stratiform environment with large widths: in most cases reflectivity factor is less than 40 dBZ. Our data exhibits no correlation between Z and SW. Very large SWs can be located in regions with $Z < 10 \text{ dBZ}$. Extremely large SW can take place at heights below 1 km. Low level layers with strong gradients of the Doppler velocity and large spectrum widths encompass flight danger because airplanes are near the ground and have relatively low speed and thus more vulnerable to wind variations. Because stratiform precipitation can last for hours, warnings based on SW could cause long delays if large SWs are along the approach and departure corridors, and these are deemed to be potential for unsafe flight.

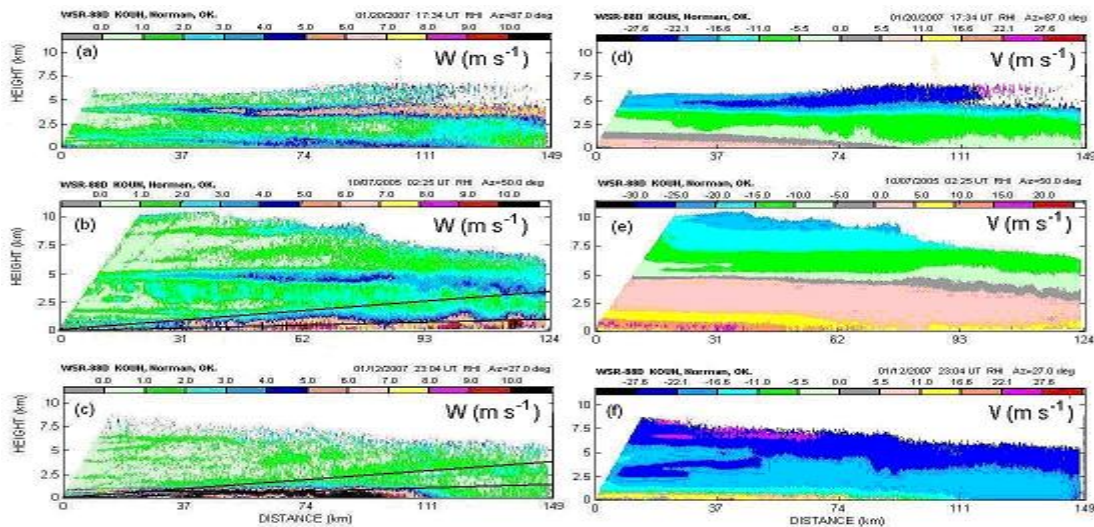


Fig.2. RHIs of stratiform precipitation; (a, b, c) the spectrum width fields and (d, e, f) corresponding Doppler velocities.

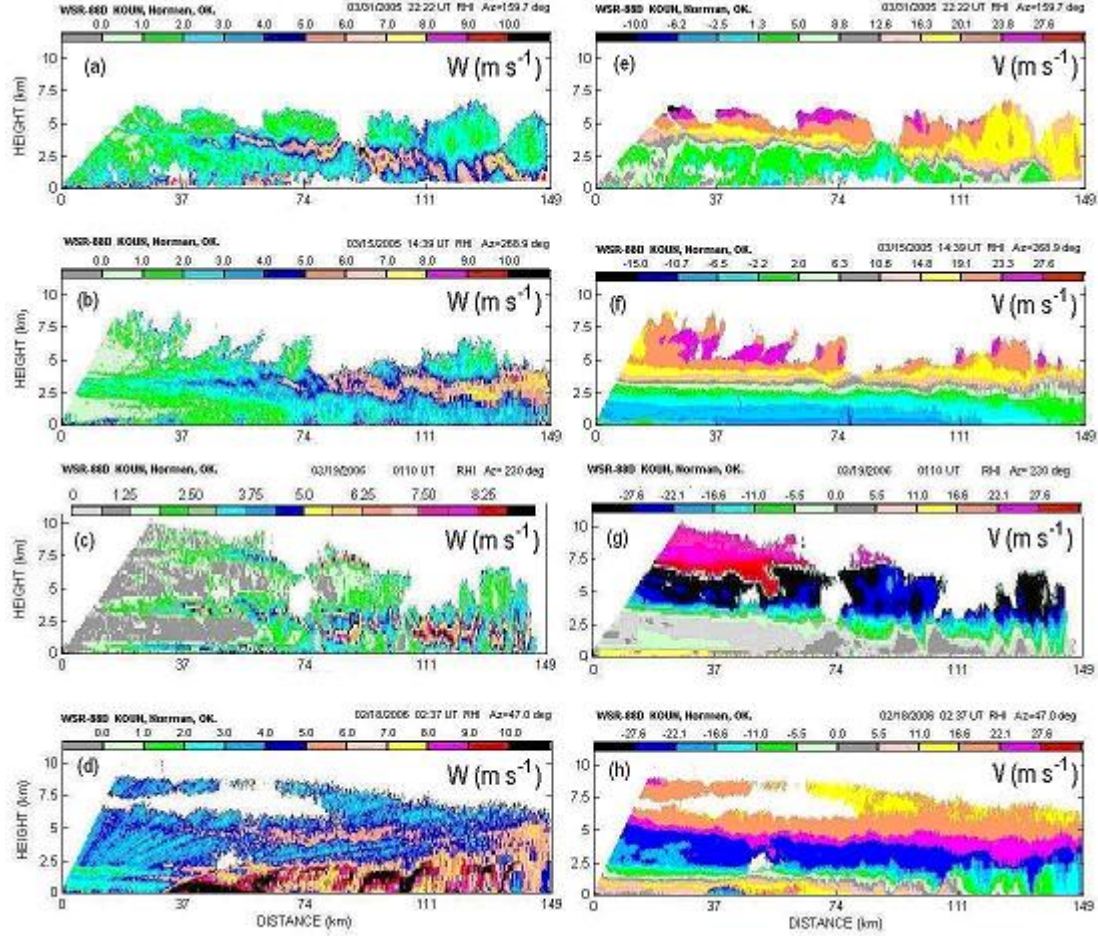


Fig. 3. Vertical cross-sections (a, b, c, d) of the spectrum width and (e, f, g, h) corresponding images of the Doppler velocities exhibiting strong wavy patterns.

Our observations show that layers with large widths can have wave-like patterns with amplitude ranging from less than 0.5 to about 2 km. Examples are shown in Fig. 3. In Fig. 3d, it is difficult to label the SW field as wave-like: it is rather chaotic with extremely large widths. Due to the high spatial variability of the velocity and extremely large values of SWs, such zones are probably very dangerous for flights, at least to the safety and comfort of the crew and passengers.

3. Estimation of mean wind shear

Images in Figs. 2 and 3 exhibit strong vertical shears of mean horizontal wind. To estimate vertical shear, height profiles of the mean wind should be measured. By definition, the vertical shear, S_v , is calculated

from mean horizontal velocities V_{H1} and V_{H2} at two heights H_1 and H_2 (i.e., $S_v = (V_{H2} - V_{H1}) / (H_2 - H_1)$). Weather radar measures the radial component of the mean horizontal wind and turbulence. Fig. 4 sketches geometry for the shear calculation: two beams at elevations θ_1 and θ_2 are shown in the figure. At point A, the vertical wind shear of horizontal wind can be estimated as

$$\hat{S}_v = \frac{(\hat{V}_B / \cos \theta_2) - (\hat{V}_A / \cos \theta_1)}{H_B - H_A}, \quad (1)$$

where $\hat{V}_{A,B}$ are the measured radial Doppler velocities (indicated by the diacriticals) which include the radial component v_r of turbulence. Because v_r is a zero mean random variable,

horizontal averages of \hat{S}_v would give the true vertical shear of mean wind. Data within a block, 500 m vertically thick and 250 m in horizontal thickness, are averaged to give at each point (i.e., block) averaged Doppler

velocities $\hat{V}_{A,B}$. At 120 km range not more than 2 data points are averaged.

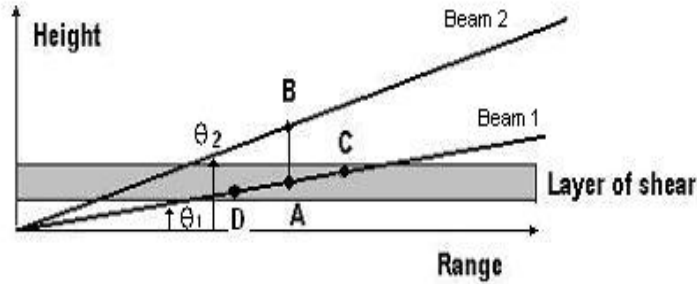


Fig. 4. Locations used to calculate mean wind shear from Doppler velocities.

Eq. (1) is a good estimation of the shear if the resolution volume V_6 at point B is inside the shear layer. If common elevation sampling (i.e., about 1°) is used, this scheme works well at short distances where V_6 at point B is likely to be within the shear layer.

Because common elevation sampling is typically too coarse to make accurate measurements of vertical shear, another scheme, one that makes use of the Doppler velocities along the beam, is proposed. For example, to calculate the shear at point A (Fig. 4), the Doppler velocities at points C and D belonging to the same radial can be utilized. In this case the vertical shear can also be obtained from

$$\hat{S}'_v = \frac{(\hat{V}_C - \hat{V}_D) / \cos \theta_1}{H_C - H_D}. \quad (2)$$

Because the errors in estimating \hat{S}'_v are an inverse function of $H_C - H_D$, the height differences should be more than one hundred meters. Because of variance in Doppler measurements, use of smaller values causes large variance in shear estimates. But at low elevations, this requires the radial distance between C and D to be a few kilometers. To simplify the preliminary analysis, we have chosen to keep the range interval C-D at 3 km. Both schemes rely on the uniformity of mean horizontal wind, but estimates could have large variance because of turbulence.

To compare these two wind shear estimation schemes, we have conducted radar observations using RHI scans with small elevation increment of 0.2° , i.e., about one fifth of the beamwidth. This estimate will be denoted as \hat{S}_v , and is considered as the true vertical shear of the mean wind. But there are fluctuations in \hat{S}_v due to turbulence. The vertical shear estimated from Doppler velocities along a single radial will be denoted as \hat{S}'_v . Fields of \hat{S}_v and \hat{S}'_v , calculated from the velocity fields shown in Fig. 2, are presented in Fig. 5. One can see that within distances of about 70 km and for not very low elevations, \hat{S}_v and \hat{S}'_v agree reasonably well, but \hat{S}'_v is slightly larger than \hat{S}_v . It is seen that at distances beyond 70 km and low elevations, \hat{S}'_v values on average are much larger than those for \hat{S}_v . There are two reasons for this. The first one is that at low elevations $H_C - H_D$ is small, and this enlarges the turbulence induced fluctuation in \hat{S}'_v as seen in Fig 5.

The second reason is related to the shape of a shear layer. This is shown in Fig. 6 for a wavy shear layer. \hat{S}_v is calculated using velocities at points A and B that are 500 m

apart whereas \hat{S}_v is calculated using velocity data 3 km apart. If both B and C are within the tilted layer, the velocity difference between D and C could be much larger because the data points are 3 km apart vs the 500 m difference for points at A and B. That is, vertical shear computed along a radial

could be enhanced by tilting of the layer. We shall consider this as overestimation of the shear because the true shear should be the change of the horizontal wind component along the vertical. That is, vertical shear estimation using data along a single radial could overestimate the vertical shear for wavy layers at low elevations.

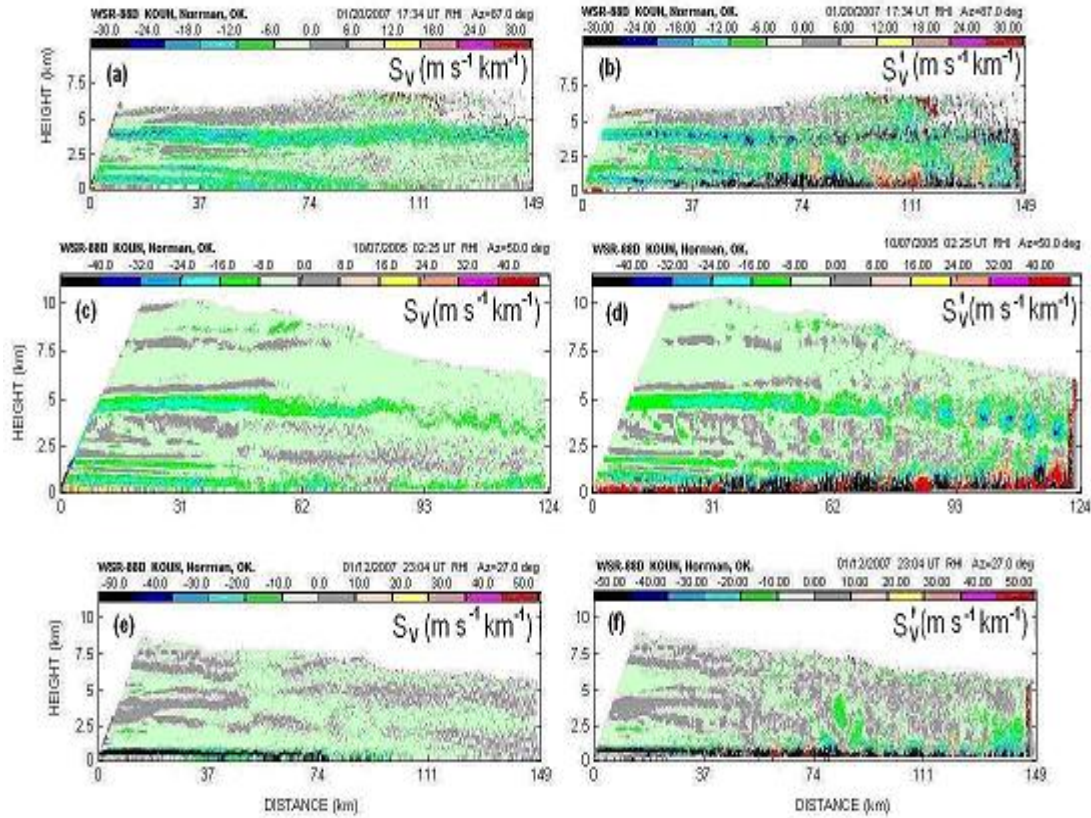


Fig. 5. (a, c, e) \hat{S}_v , and (b, d, f) \hat{S}'_v fields corresponding to velocity fields in Fig. 2.

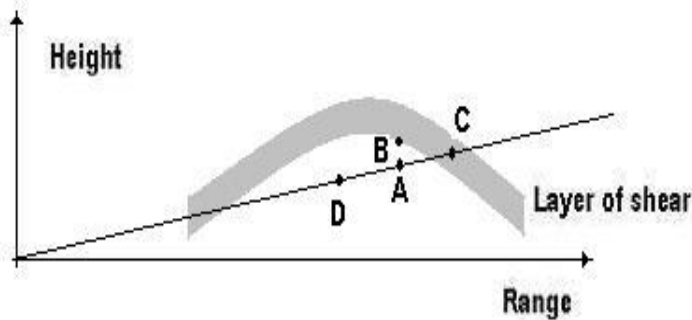


Fig. 6. Locations used to calculate mean wind shear if a wavy layer were present.

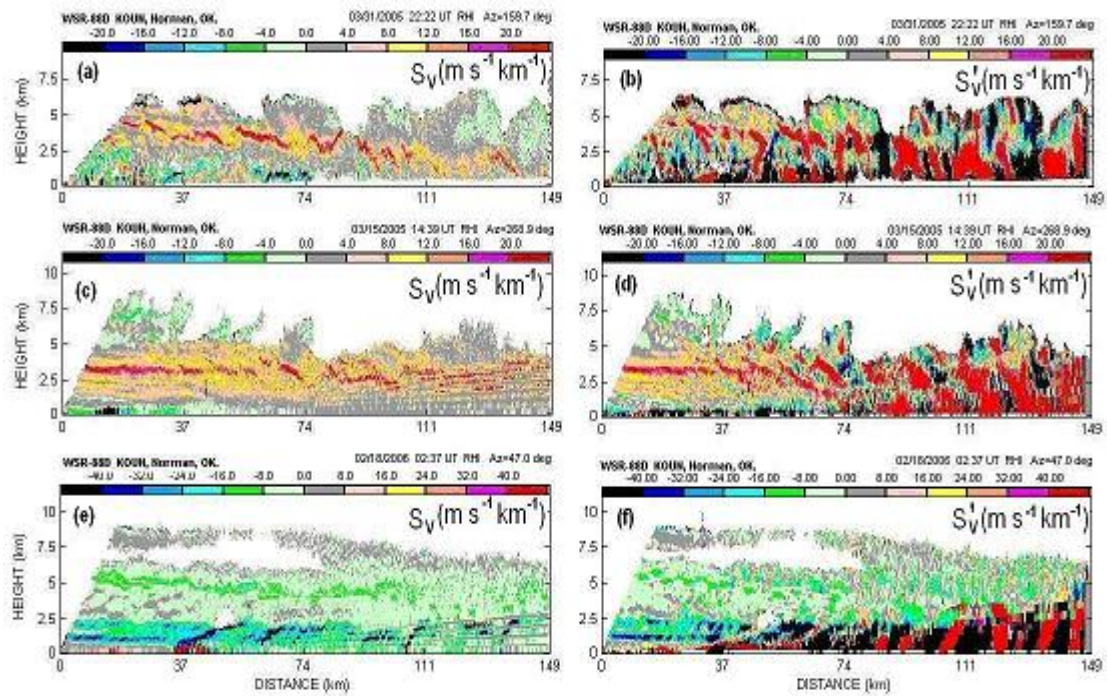


Fig. 7. (a, c, e) S_h and (b, d, f) S_s fields obtained from velocity fields in Fig. 3.

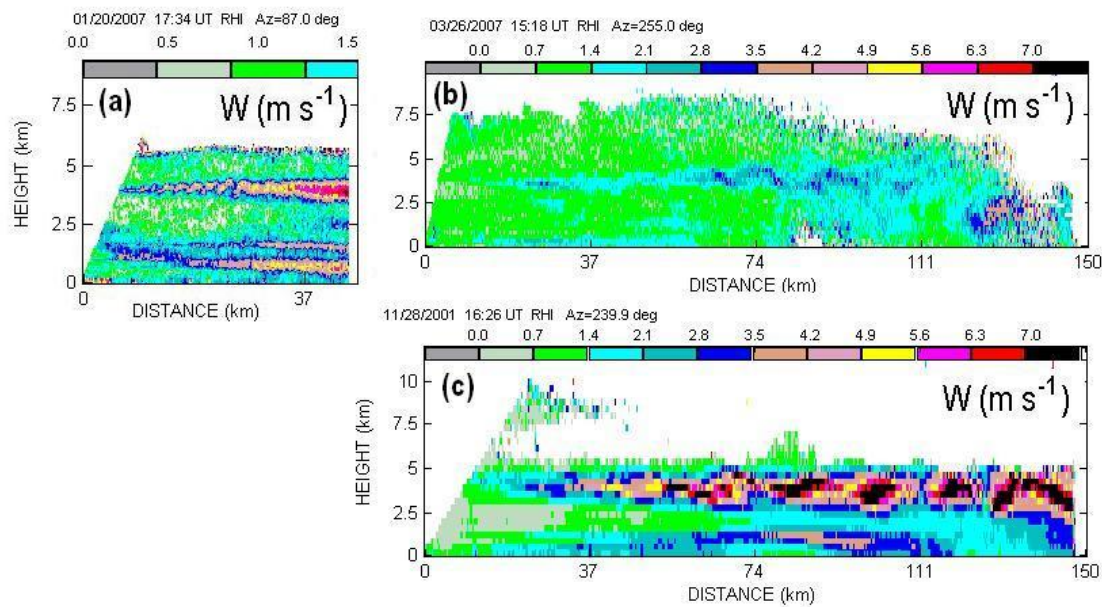


Fig.8. Spectrum width fields exhibiting wavy or periodic patterns.

Strong overestimation of the shear calculated from data along a single radial can be seen in Fig. 7 for wavy velocity fields presented in the right column in Fig. 3; Vertical shear estimates \hat{S}'_v become anomalously large at ranges beyond about 30 km.

Beyond about 70 km, both S_v and S'_v estimators exhibit reduced performance at low heights above ground because of earth's curvature, the larger vertical distance between the beams, and the larger beamwidth. For such cases, spectrum width could be a better estimate of the wind shear because it is measured at each V_6 (i.e., there is no need for Doppler velocities at two heights). But SW combines the wind shear and turbulence contributions (Doviak and Zrníc, 2006). Because both turbulence and shear are a potential hazard to low flying aircraft, SW might be a better estimate to gauge the safety of flight at low altitudes.

Our data show that layers of large S_v , S'_v and SW can be very thin. For example, the thickness of wind shear layers in Figs. 2 (c) and 8 (a) were estimated to be less than 500 m (i.e., the vertical resolution of the interpolation box). Estimated wind shears in Figs. 5(e) and 7(e) are over $60 \text{ m s}^{-1} \text{ km}^{-1}$. Such strong wind shears in the approach and departure corridors near the ground makes them dangerous for safe flights.

Often, S_v and S'_v fields exhibit wavy or spatially periodic patterns. Waves in the S_v field are seen in Fig. 5(c) at heights of 3 to 4.5 km and at distances beyond 80 km. Corresponding velocity field in Fig. 2(e) is wavy as well. In the same area, S'_v (Fig. 5d) looks like a periodic pattern. Periodic patterns in S_v and S'_v fields are seen in Figs. 5(a,b) at about 4 km height and distances within 30 km. Such structures are often difficult to discern in the Doppler velocity fields (e.g., Fig. 2d). But they are more frequently visible

in the SW field (e.g., Fig. 8a; this is a part of Fig. 2(a) in different color legend to highlight the wave). The wave has maximal amplitude of about 0.5 km and a wavelength of 2.5 km. Very pronounced wavy patterns in the Doppler fields are seen in Fig. 3. Spatial periodicity in the S_v and S'_v fields can also be noted in Figs. 7 (a,b,c,d).

Wavy and periodic patterns are demonstrated in other SW fields. For example, Fig. 8(b) shows a wave at heights from 3 to 4.5 km at distances 50 to 90 km. Note that Fig. 8 (b) is the same date of stratiform precipitation shown in Fig.1, i.e., waves can occur in stratiform precipitation with small SWs. A periodic patchy SW pattern is presented in Fig. 8(c). This pattern suggests the presence of Kelvin-Helmholtz waves. These waves usually have periodical vertical wind velocities with amplitudes 1 to 3 m s^{-1} (Chapman and Browning, 1999; Hogan et al., 2002). So the presence of waves in SW or $S_{h,s}$ fields can serve as an indicator of the existence of periodic vertical winds which can cause unpleasant aircraft accelerations. Our radar data show that the waves can be observed in precipitation with both strong and weak wind shears.

4. Conclusions

- Radar observations of spectrum width fields, SW, in stratiform precipitation frequently exhibit the presence of areas with SW larger than 4 m s^{-1} (more than 80% of the analyzed cases), which according to research findings in thunderstorms corresponds to moderate or strong turbulence as it affects aircraft (i.e., derived gust velocities exceed 6.1 m s^{-1}). SWs in stratiform precipitation often exceed 7 m s^{-1} and can reach 17 m s^{-1} , i.e., extremely large values not observed in thunderstorms. Regions of large spectrum widths more often exhibit layered patterns (more than 70% of the cases).

- In more than 40% of the cases, areas of large SW are located in the lowest kilometer from the ground. Layers of large

SW can be very narrow, i.e., less than 500 m, and the wind shears in the layers can reach $60 \text{ m s}^{-1} \text{ km}^{-1}$.

- Dense elevation sampling in radar data collection allows restoring fine structures of layers with large SW and calculating the vertical shear of the mean wind. Estimates of the vertical shear of mean wind using data along a single radial is often overestimated at low elevations. At distances beyond 70 km and low elevations, spectrum width measurements can be a good proxy to estimate wind shears.

- Often, fields of the wind shears and SW exhibit wavy or spatially periodic patterns which are a manifestation of Kelvin-Helmholtz waves. Wavy patterns have been observed in layers with small and large SW. Such patterns can serve as an indicator of the presence of periodic vertical winds which could affect safety of flight.

References

- Bieringer, P. E., B. Martin, B. Collins, and J. Shaw, 2004: Commercial aviation encounters with severe low altitude turbulence. *Proc. 11th Conf. on Aviation, Range and Aero. Meteorol.*, Paper #11.3, 8 pp.
- Chapman, D., and K. A. Browning, 1999: Release of potential shearing instability in warm frontal zones. *Quart. J. Royal Meteor. Soc.*, **125**, 2265-2288.
- Cornman, L. B., J. Williams, G. Meymaris, and B. Chorbajian, 2003: Verification of an airborne Doppler radar turbulence detection algorithm. *Sixth Int. Symp. Tropospheric Profiling*, Leipzig, Germany, German Weather Service, 9-11.
- Doviak, R. J. and D. S. Zrnic, 1993: *Doppler Radar and Weather Observations*, 2nd ed., Academic Press, 562 pp.
- Evans, J. E., 1985: Weather Radar Studies, Dept. of Transp. report "DOT/FAA-PM-85-16", 48 pp.
- Fang, M., 2003: Spectrum width statistics of various weather phenomena and comparison of observations with simulations. *MS thesis*, University of Oklahoma, 173 pp.
- Fang, M., R. J. Doviak, and V. M. Melnikov, 2004: Spectrum widths measured by WSR-88D: Error sources and statistics of various weather phenomena. *J. Atmos. Oceanic Technol.* **21**, 888-904.
- Hamilton, D. W., and F. H. Proctor, 2002: Convectively induced turbulence encounters during NASA's 2000 fall flight experiments. *10th Conf. Aviation, Range, and Aerospace Meteorology*, AMS, 371-374.
- Hamilton, D. W., and F. H. Proctor, 2006: Progress in the development of an airborne turbulence detection system. *12th Conf. Aviation, Range, and Aerospace Meteorology*, AMS, P6.5.
- Hamilton, D. W., and F. H. Proctor, 2006: Airborne turbulence detection system certification tool set. *44th AIAA Aerospace Sciences Meeting*. Reno, Nevada, paper: AIAA 2006-75.
- Hogan, R. J., P.R. Field, A.J. Illingworth, R.J. Cotton and T.W. Choularton, 2002: Properties of embedded convection in warm frontal mixed-phase cloud from aircraft and polarimetric radar. *J. Royal Meteorol. Soc.*, **128**, 451-476.
- Istok, M. J., and Doviak R. J., 1986: Analysis of the relation between Doppler spectra width and thunderstorm turbulence. *J. Atmos. Sci.*, **48**, 2199-2214.
- Lee, J. T., 1977: Application of Doppler radar to turbulence measurements which affect aircraft. *Federal Aviation Administration Reports*. RD-77-145, 11 - 19.
- Mahapatra, P., 1999: *Aviation Weather Surveillance Systems*. IEE Radar, Sonar, Navigation, and Avionics Series 8., Co-publishers: IEE and AIAA, 458 pp.
- Meischner P., R. Bauman, H. Holler, T. Jank. 2001: Eddy dissipation rates in thunderstorms estimated by Doppler radar in relation to aircraft *in situ* measurements. *J. Atmos. Ocean. Technol.*, **18**, 1609-1627.
- Proctor, F. H., D. W. Hamilton, and R. L. Bowles, 2002: Numerical simulation of a convective turbulence encounter. *10th Conference ARAM*, pp. 41-44.